Eur Biophys J (2000) 29: 165–171

ARTICLE

Marina Zelenina · Hjalmar Brismar

Osmotic water permeability measurements using confocal laser scanning microscopy

Received: 12 June 1999 / Revised version: 21 February 2000 / Accepted: 25 February 2000

Abstract We have developed a method for measurement of plasma membrane water permeability (P_f) in intact cells using laser scanning confocal microscopy. The method is based on confocal recording of the fluorescence intensity emitted by calcein-loaded adherent cells during osmotic shock. P_f is calculated as a function of the time constant in the fluorescence intensity change, the cell surface-to-volume ratio and the fractional content of the osmotically active cell volume. The method has been applied to the measurement of water permeability in MDCK cells. The cells behaved as linear osmometers in the interval from 100 to 350 mosM. About 57% of the total cell volume was found to be osmotically inactive. Water movement across the plasma membrane in intact MDCK cells was highly temperature dependent. $HgCl_2$ had no effect on water permeability, while amphotericin B and DMSO significantly increased P_f values. The water permeability in MDCK cells transfected with aquaporin 2 was an order of magnitude higher than in the intact MDCK cell line. The water permeability of the nuclear membrane in both cell lines was found to be unlimited. Thus the intranuclear fluid belongs to the osmotically active portion of the cell. We conclude that the use of confocal microscopy provides a sensitive and reproducible method for measurement of water permeability in different types of adherent cells and potentially for coverslip-attached tissue preparations.

Key words Aquaporins · MDCK cells · Water permeability · Cell volume · Laser scanning confocal microscopy

M. Zelenina (✉) · H. Brismar
Department of Woman and Child Health,
Q2: 09 Astrid Lindgren Children's Hospital,
Karolinska Institutet, 171 76 Stockholm, Sweden
e-mail: marina.zelenina@ks.se

M. Zelenina
Laboratory of Physiological Genetics,
Institute of Cytology and Genetics, 630090 Novosibirsk, Russia

Introduction

Water movement across the plasma membrane can occur via two pathways: by diffusion through the lipid bilayer (Finkelstein 1987) and via membrane-inserted water channels (aquaporins) (King and Agre 1996; Knepper et al. 1997; Sasaki et al. 1998). The number of identified members of the aquaporin protein family is persistently growing (Park and Saier 1996). Since the main feature of these proteins is their ability to transport water across the membranes, the characterisation of aquaporin function, abundance, regulation pathways, tissue- and cell-specific distribution necessarily involves quantitative studies of aquaporin-expressing cell membrane water permeability.

Aquaporins account for an *osmotic* water permeability of cell membranes, which is significantly higher than the *diffusional* water permeability accounted for by water conductance of the membrane lipid bilayer. One of the main parameters in the characterisation of osmotic water permeability is the osmotic water permeability coefficient, P_f (Verkman et al. 1996). All known methods for P_f measurements in living cells or membrane vesicles are based on a common principle: cells, tissue or vesicle preparations are exposed to hypo- or hyperosmotic shock, and the time course of the changes in cell/vesicle volume or in marker compound concentration is registered. Methods based on cell volume monitoring are more widely used compared to tracing of a marker compound, since they are usually faster and do not need the use of radioactivity.

Changes in cell volume can be monitored either through direct observation of the cell geometry (Lopes and Guggino 1987; Oliet and Bourque 1993; Roberts et al. 1994; Yano et al. 1996; Zhang et al. 1990), or through registration of changes in fluorescence intensity emitted by fluorescent dye-loaded (or labelled) cells. The latter group of techniques is more often used, since it can be applied to a wider spectrum of cell preparations. Within this group, the techniques differ mostly by the

method of registration of the emitted fluorescence, which to a great extent determines the accuracy of the P_f measurements and the type of biological samples the method can be used for.

Here we present a technique for real-time monitoring of changes in cell volume based on confocal imaging of living cells loaded with a membrane-impermeable fluorescent dye. The suggested method combines most of the advantages and overcomes certain limitations in previously described methods. The method can be used for osmotic water permeability quantification in different types of adherent cells and potentially for coverslip-attached tissue preparations.

Materials and methods

Cell culture and loading

MDCK cells (ICN Biomedicals Europe; purchased from In Vitro Biomedical Products, Stockholm, Sweden; subpassages 3–16) were grown on round glass coverslips (40 mm diameter, Bioptechs, Butler, PA, USA) in minimum essential medium (MEM) containing 2 mM L-glutamine and supplemented with 10% (vol/vol) fetal calf serum (FCS) at 37 °C in 5% CO_2.

MDCK cells transfected with aquaporin 2 (AQP2) (clone WT-10) were kindly provided by Dr. Peter M.T. Deen (University of Nijmegen, The Netherlands) (Deen et al. 1997). The cells were grown in DMEM containing 25 mM HEPES, 4.5 g/l glucose, 2 mM L-glutamine and supplemented with 5% (vol/vol) FCS at 37 °C in 5% CO_2.

Both MDCK and WT-10 cells were used at 80–90% confluence. Dye loading was carried out as described (Farinas et al. 1995). Briefly, the cells were rinsed with PBS (in mM: 137 NaCl, 0.9 $CaCl_2$, 0.49 $MgCl_2$, 2.7 KCl, 1.5 KH_2PO_4, 8.1 Na_2HPO_4, pH 7.35) and incubated for 30 min at 37 °C in corresponding culture medium containing 5 μM of the fluorescent dye calcein-AM (Molecular Probes Europe, Leiden, The Netherlands). Calcein-AM was added to the medium just before use from a 10-mM stock solution in DMSO. Following dye loading, the coverslips were rinsed with PBS. In some experiments, calcein-loaded cells were rinsed with PBS and incubated in MEM containing 0.5 mg/ml amphotericin B for 10 min at 37 °C in 5% CO_2/95% air. Amphotericin B was added from a 25-mg/ml stock solution in DMSO just before use. To the control cells, only vehicle (DMSO) was added. After incubation the cells were rinsed with PBS.

Data acquisition and analysis

Coverslips with calcein-loaded cells were mounted in a closed perfusion chamber (Focht Live Cell Chamber System, Bioptechs, Butler, PA, USA) on the stage of a Zeiss 410 invert laser scanning microscope (LSM). Perfusion solutions were gravity pumped (flow rate approximately 5 ml/min) and switched using two-way valves.

PBS (300 mosM) was used for isoosmotic perfusion. Anisoosmotic solutions were prepared by varying the PBS NaCl content (187, 162, 87, 62, and 37 mM NaCl for 400, 300, 200, 150, and 100 mosM solutions, respectively). In experiments with $HgCl_2$ the chemical was present both in iso- and anisoosmotic perfusion solutions at a concentration of 0.3 mM.

Images were recorded by the LSM using a 63×/1.4 oil immersion objective. Fluorescence was excited by the argon laser line 488 nm and emitted fluorescence was detected using a bandpass filter at 515–525 nm. The focal plane was set at a distance of about 1/3 of the cell height from the bottom of cell monolayer.

Square-shaped regions of interest (ROIs) were set inside the cytoplasmic area of several (up to 10) cells, and the mean intensity within the ROIs was recorded every 2 s. At the beginning of the measurements, the standard deviation of the fluorescence intensities between individual cells did not exceed 15%.

The cells were perfused by isotonic PBS for at least 10 min before confocal scanning and during the first 50 s of data acquisition. The linear slope of this first part of the intensity curve was used for photobleaching and leakage correction.

The part of the recorded intensity curve corresponding to the first 20 s after osmotic shock was fitted with a single exponential function and used for calculation of the time constant of the fluorescence intensity changes (see below). The part of time course corresponding to the steady state before the regulatory volume decrease was used for the calculation of the final relative volume for the calibration curve.

Cell surface and volume measurement

Calcein-loaded cell monolayers were scanned with a focus displacement of 0.2–0.4 μm. Recorded stacks of images were processed using the Imaris image processing toolkit (Bitplane, Zurich, Switzerland) on a Silicon Graphics workstation. Cells were outlined in consecutive images ranging from the bottom to the top of the cells. Both the surface area and the volume of the outlined geometric objects were calculated automatically by the software.

P_f calculation

P_f was calculated by the following formula (Farinas et al. 1995):

$$P_f = [d(F/F_0)/dt](1 - b/V_0)[\gamma(A/V)_0 V_w \Delta\phi_0]^{-1} \quad (1)$$

where (F/F_0) is the relative fluorescence intensity, $[d(F/F_0)/dt]$ is the initial rate of the relative fluorescence intensity changes during cell swelling/shrinkage in response to an osmotic shock, $(1-b/V_0)$ represents an

osmotically active portion of cell volume, γ is the slope of the calibration curve (relative fluorescence versus relative osmolarity), $(A/V)_0$ is the initial cell surface-to-volume ratio (in cm^{-1}), V_w is the partial molar volume of water (18 cm^3/mol), and $\Delta\phi_0$ is the initial osmotic gradient (outside − inside) (in mol/cm^3).

Data analysis and statistics

The photobleaching correction, exponential curve fitting and statistical analyses were performed using Microsoft Excel and KaleidaGraph (Abelbeck Software, USA). Data are presented as means ± SE. Statistical analyses were made using Student's *t*-test. A difference of $P < 0.05$ was considered statistically significant.

Results

As follows from Eq. (1), determination of the osmotic water permeability coefficient requires quantification of several parameters. First, it is necessary to record the changes in the relative fluorescence intensity emitted by the intracellularly trapped fluorophore (F/F_0) which follow the changes in cell volume during response to an osmotic shock.

In the suggested method, the fluorescence intensity is measured in a thin (less than 0.5 μm) layer inside the cell. Figure 1B shows the typical time course of fluorescence intensity before and after hypoosmotic shock (open circles). Although the intensity of the excitation light was attenuated to a minimum value, the emitted fluorescence slightly decreased over the time of the experiment owing to calcein photobleaching and/or leakage from the cells. Each time course of cell swelling was therefore corrected using the linear slope of the first part (about 45 s, 20 recordings) of the curve just before the osmotic shock (Fig. 1B, solid circles).

The part of the corrected curve (about 20 s) following the change of perfusate osmolarity was fitted by a single exponential function

$$y = \alpha + \beta\, e^{-\tau x} \tag{2}$$

From this function the exponential time constant τ was used in Eq. (1) as the measure of the rate of osmotic cell swelling:

$$P_f = \tau(1 - b/V_0)[\gamma(A/V)_0 V_w \Delta\phi_0]^{-1} \tag{3}$$

The part of the corrected curve (Fig. 1, white bar) corresponding to maximal cell swelling before regulatory volume decrease (or to maximal cell shrinkage before regulatory volume increase in the case of hyperosmotic shock) was used for plotting a calibration curve representing the dependence between relative osmolarity ϕ/ϕ_0 and relative fluorescence F/F_0 (Fig. 2). The curve fitting of the obtained data (solid line) shows that the cells behave as linear osmometers, at least in response to hypoosmotic shock. This means that changes in relative fluorescence are linearly dependent on the changes in relative osmolarity over a wide range of initial osmotic

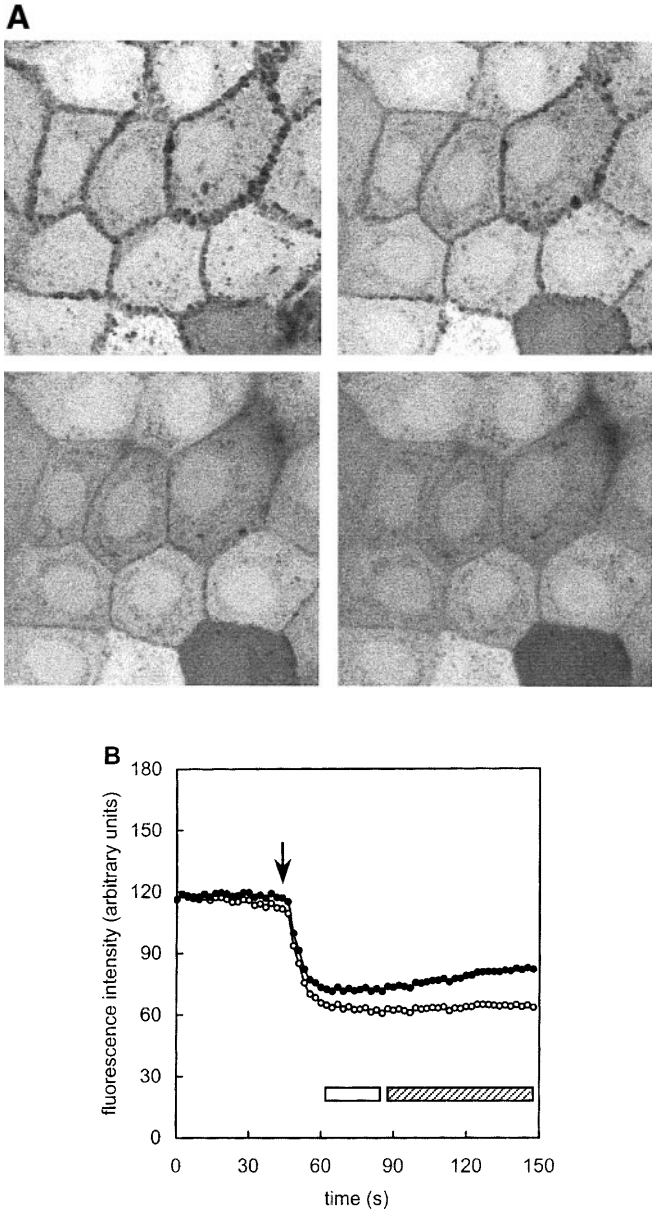

Fig. 1A Confocal micrographs of calcein-loaded MDCK cells under osmotically induced volume changes. Images are from 0, 6, 12 and 18 s after changing the isotonic (300 mosM) superfusion solution 1 to hypoosmotic (150 mosM) solution 2. Entire cells, including nuclei, are loaded with the fluorescent dye. As the cells swell, the fluorescence intensity in the cytoplasm and nuclei decreases. The cell swelling occurs not only in the apical but also in the lateral direction, and the intracellular spaces disappear. **B** Representative time course of fluorescence intensity emitted by calcein-loaded MDCK cells before and after hypoosmotic shock. The *arrow* indicates the time when the isoosmotic superfusion solution has been changed to hypoosmotic. (○) Raw data; (●) curve corrected for calcein photobleaching and/or leakage of the dye from the cell. The w*hite bar* indicates the period of maximal cell swelling; the *shaded bar* indicates the regulatory volume decrease

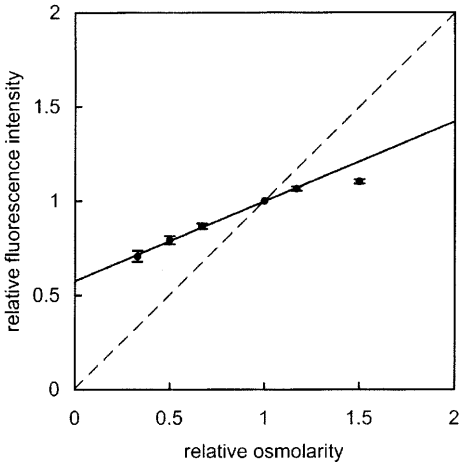

Fig. 2 Dependence of relative intensity (F/F_0) of the fluorescence emitted by calcein-loaded MDCK cells on the relative osmolarity (ϕ/ϕ_0) of the superfusion solution. Relative osmolarity is calculated as the osmolarity of solution 2 (see legend to Fig. 1) divided by the osmolarity of solution 1. Relative fluorescence intensity is calculated as the mean intensity during a period of maximal swelling (Fig. 1) related to the initial fluorescence of the cell just before the solution change. Values are means ± SE of 17–28 cells. *Solid line*: linear fitting of experimental data; *dashed line*: behaviour of ideal osmometer. Cells behave as linear osmometers in a wide osmolarity range. The difference between the experimental data and the behaviour of an ideal osmometer implies that part of the cell volume is osmotically inactive

gradients. The change in the osmolarity of the superfusing solution from 300 mosM to 150 mosM was chosen for further P_f measurements. The slope of the obtained fitting line was used in Eq. (3) as a mean for γ.

The experimentally obtained dependence between relative osmolarity ϕ/ϕ_0 and relative fluorescence F/F_0 differs substantially from the behaviour of an ideal osmometer (Fig. 2, dashed line). This suggests that only part of the cell volume is osmotically active.

Estimation of the osmotically inactive portion of the cell is necessary for the P_f calculation. In Eq. (1) and (3) the osmotically inactive part of the cell volume is represented by b/V_0. This factor has been believed to be the fractional content of cell solids, and in some reports, b has been set to zero to simplify calculation of P_f (Farinas et al. 1995; Valenti et al. 1996). However, with the use of Boyle-van't Hoff plot analysis it has been reported that the osmotically inactive component of the cell volume is approximately 20% of the total volume in rabbit kidney proximal tubular cells (Meyer and Verkman 1987) and about 50% in human sperm (Gilmore et al. 1995). Moreover, b/V_0 obviously represents not only cell solids, but also osmotically inactive water (about 8–9% of total cell volume) (Gilmore et al. 1995).

The use of confocal microscopy and cell shape reconstruction allows estimation of the osmotically inactive portion of the cell volume using the following equation (Farinas et al. 1995):

$$(V_0 - b)/(V - b) = \phi/\phi_0 \quad (4)$$

where b is the osmotically inactive cell volume, V_0 the initial cell volume, V the cell volume after swelling, ϕ_0 the initial osmolarity of solution and ϕ the final osmolarity. Replacing ϕ/ϕ_0 with ϕ_r (relative osmolarity), we get:

$$b = (V_0 - \phi_r V)/(1 - \phi_r), \quad (5)$$

and

$$b/V_0 = (V_0 - \phi_r V)/[(1 - \phi_r)V_0] \quad (6)$$

Thus, the osmotically inactive part of the cell volume can be determined from cell volume measurements before (V_0) and after (V) the change of perfusate osmolarity.

The same calcein-loaded cells were scanned in isoosmotic conditions and 20 s after the solution switch. The acquisition of one stack of images took about 40 s and could be completed before the start of the regulatory volume decrease. The obtained volume data for $\phi_r = 0.5$ (osmolarity change from 300 to 150 mosM) gave b/V_0 equal to 0.57 ± 0.04 ($n = 7$). This means that about 57% of the MDCK cell volume is osmotically inactive, and only about 43% of the cell volume participates in the response to acute hypoosmolarity. The intranuclear fluid belongs to osmotically active cell volume (see below).

The scanning of the cells in isotonic conditions and subsequent cell volume and surface area calculations allowed us to determine the initial cell surface-to-volume ratio $(A/V)_0$. For the MDCK cell monolayers this was found to be 6920 ± 460 cm^{-1} ($n = 7$).

The mean values for $(1-b/V_0)$, γ and $(A/V)_0$ calculated for MDCK cell monolayers were used for calculation of P_f in further experiments designed to evaluate the suggested method of cell volume measurements.

As shown in Fig. 3, water movement across the membranes of MDCK cells is temperature-dependent. P_f is 1.01 ± 0.43 × 10^{-4} cm/s ($n = 22$) at 15 °C, and 2.73 ± 0.26 × 10^{-4} cm/s ($n = 21$) at 24 °C ($P < 0.01$).

It is known that mercurials inhibit water permeability of most aquaporins (Wintour 1997). In our experiments, $HgCl_2$ had no effect on water permeability in MDCK cells (data not shown). The low P_f values, the absence of a $HgCl_2$ effect, as well as the high temperature dependence of P_f suggest the absence of significant amounts of water channels in MDCK cells. These data correspond well to previous observations suggesting that, in this cell line, water permeates the plasma membrane mostly through the lipidic phase of the membrane (Giocondi et al. 1990).

Amphotericin B, which forms artificial pores in the plasma membrane (Fournier et al. 1998), significantly ($P < 0.001$) increased P_f in MDCK cells (Fig. 4). In the presence of 0.3 mg/ml amphotericin B, P_f was found to be 6.15 ± 0.59 × 10^{-4} cm/s ($n = 18$), while in control cells treated with vehicle (DMSO) it was 3.61 ± 0.21 × 10^{-4} cm/s ($n = 20$). DMSO itself has a pronounced effect on water permeability ($P < 0.05$),

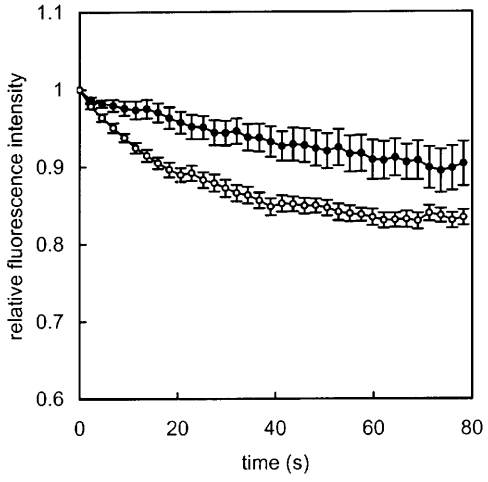

Fig. 3 Plasma membrane water permeability of MDCK cells is highly temperature dependent. Calcein-loaded cells were superfused by an isoosmotic (300 mosM) solution which was changed to a hypoosmotic (150 mosM) solution at time point 0. Data were recorded at 24 °C (○) and 15 °C (●). Values are means ± SE of 21 and 22 cells, respectively

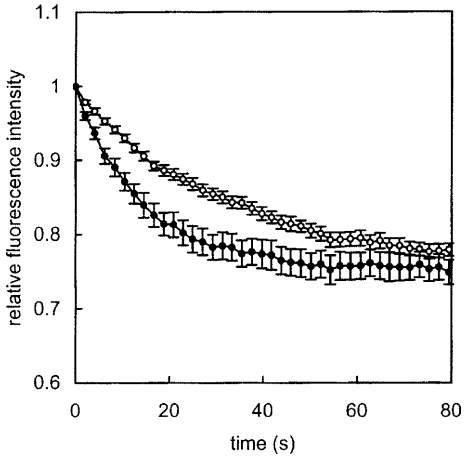

Fig. 4 Amphotericin B significantly increases plasma membrane water permeability in MDCK cells. (●) Amphotericin B (0.3 mg/ml); (○) vehicle (DMSO). Values are means ± SE of 18 and 20 cells, respectively

probably due to its solvation effects on the phospholipid structure of the cellular membranes (Yu and Quinn 1998).

In transfected MDCK cells expressing aquaporin 2 (WT-10 clone; Deen et al. 1997), the water permeability is dramatically increased compared to ordinary MDCK. P_f is $24.39 \pm 0.94 \times 10^{-4}$ cm/s ($n = 55$) in transfected and $2.32 \pm 0.12 \times 10^{-4}$ cm/s ($n = 51$) in nontransfected cells ($P < 0.001$) (Fig. 5).

The rate of fluorescence intensity change measured in nuclei of both WT-10 and MDCK cells, under different experimental conditions, was the same as in the cytosol (data not shown). This indicates that the water permeability of the nuclear membrane is high and the intranuclear fluid effectively participates in osmotic cell volume changes. The nuclear membrane permits free

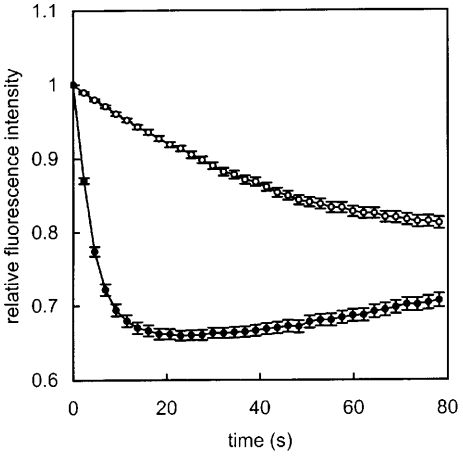

Fig. 5 MDCK cells transfected with the aquaporin 2 water channel (WT-10 clone; Deen et al. 1997) have significantly higher water permeability than non-transfected cells. (●) WT-10 cells; (○) MDCK cells. Values are means ± SE of 55 and 51 cells, respectively

water transport, probably due to the nuclear pores perforating the nuclear envelope (Alberts et al. 1994).

Discussion

The critical factor in determining P_f in living cells is the method used to measure the rate of cell volume change in response to an osmotic shock.

Several methods for cell volume monitoring have been developed during the last two decades. Direct measurement of the cell linear size from light microscopy images has been used in studies of cell suspensions, renal tubule preparations or in model systems like frog oocytes (Lopes and Guggino 1987; Roberts et al. 1994; Yano et al. 1996; Zhang et al. 1990). This approach has also been used for single adherent cells (Oliet and Bourque 1993), although it is applicable only for cells with a geometrically even shape.

Fluorescence quenching and light scattering methods are mostly used for P_f measurements in liposomes and vesicles (Chen et al. 1988; van Heeswijk and van Os 1986). Light scattering can also be used for measurements in cultured cells (Echevarria and Verkman 1992; Fischbarg et al. 1989; McManus et al. 1993), although this method has several potential problems in quantitative data interpretation (Verkman et al. 1996). Fluorescence quenching techniques have recently been used for cell volume monitoring in cell cultures, but the use of this method might be restricted by ion sensitivity of the fluorophores used (Srinivas and Bonanno 1997).

Some other methods for recording cell swelling/shrinkage have been established, based on single fluorescent particle tracking (Kao and Verkman 1994), electronic particle counting (Gilmore et al. 1995), laser interferometry (Farinas and Verkman 1996) and on light microscopy with spatial filtering (Farinas et al. 1997).

The method suggested here is based on the recording of swelling/shrinkage related changes in the fluorescence intensity of intracellularly trapped membrane-impermeable fluorescent dyes. Two methods using the underlying principle have been established so far. Fluorescence video microscopy implies the imaging of fluorophore-loaded cells with subsequent analysis of image intensity data (Crowe et al. 1995; Tauc et al. 1990). Total internal reflection (TIR) microfluorimetry uses the quantification of the fluorescence emitted by the evanescent field in a thin layer of cytosol adjacent to the glass-aqueous interface (Farinas et al. 1995).

The limitation of fluorescence video microscopy as a method for cell volume measurements is that it collects the emitted light from a layer comparable to the cell height. When thin cell monolayers are used, the thickness of the layer may even exceed the cell height. Then, as the cell is swelling, the decrease of fluorescence intensity in the cytoplasm is neutralised by the increase in cell height. Simple geometric consideration leads to the conclusion that, if the relative change in cell volume is the same, the thinner cell will demonstrate more relative change in its height, and the effect of cell height increase on the general change of fluorescent intensity will be more significant in the thinner cell. This means that cell volume measurements using fluorescence video microscopy are dependent on cell shape, and therefore on cell line and confluency of the cell culture.

TIR microfluorimetry overcomes the limitation of fluorescence video microscopy by recording the fluorescence intensity from a thin cell layer adjacent to a coverslip. However, it is well known that the basal membrane of the cell represents a complex-profiled surface with grooves and convexities (Alberts et al. 1994). In our experiments, we observed that even in confluent monolayers growing on coverslips there is much free space under and between the cells, particularly in the regions underlying tight junctions. In some cell lines (especially after transfections disturbing cell attachment properties) the cells can have rather small areas contacting a coverslip and a lot of space between the cell basal membrane and the glass surface (M. Zelenina, unpublished observations). This space may contain a significant amount of fluorescent dye entrapped there during the loading procedure and as a result of leakage from the loaded cells. Fluorescence emitted by the entrapped dye causes artefacts disguising the true signal related to cell volume changes. The use of TIR microfluorimetry for cell volume measurements is therefore not correct for all types of cells. Furthermore, the TIR microfluorimetry method can be difficult to use in heterogeneous cell populations.

Confocal microscopy for cell volume measurement combines the advantages and overcomes the limitations of fluorescence video microscopy and TIR microfluorimetry. Fluorescent light emitted by intracellularly entrapped fluorophores is collected from a thin layer within the cell, so that the measurements are not affected by any fluorophore that might be entrapped between and under the cells. In the described experimental conditions, the thickness of the scanned layer was less than 10% of the initial cell height. The measured intensity of the emitted light does not depend on cell shape changes during swelling/shrinkage and on the cell growth manner. Furthermore, the amount of the fluorophore subjected to excitation light during the scanning is small enough to avoid massive effects of photobleaching, as the fluorophore is rapidly replenished from the surrounding intracellular space.

The described method can easily be used in heterogeneous cell cultures, since the area chosen for analysis is precisely controlled. It can also be applied to measurements of the water permeability of membranes forming intracellular structures like vacuoles, as the chosen ROI can be small compared to the cell size. The method is potentially applicable in studies of water permeability on immobilised and perfused tubular structures, such as kidney tubules, small blood vessels, bronchioli, etc., as well as on preparations from plants. It might also be used for separate P_f measurements of apical and basolateral membranes in cells grown on porous support or in tubules perfused/superfused by anisoosmotic solution.

We conclude that confocal laser scanning microscopy provides a sensitive and reproducible method for the measurement of water permeability that can be used in different types of living cells.

Acknowledgements The authors thank Dr. Peter M.T. Deen (Department of Cell Physiology, University of Nijmegen, Nijmegen, The Netherlands) for providing the cells transfected with aquaporin 2 (WT-10 clone). We are grateful to Eivor Zettergren for cell culture preparation for all cell measurements. M.Z. thanks Dr. Ardan Patwardhan (Royal Institute of Technology, Stockholm, Sweden) for technical and mathematical support at the start of the work, and Dr. Takako Matsubara for the introduction to fluorescence microscopy. This work was supported by grants from the Swedish Medical Research Council (03644), the Swedish Heart-Lung Foundation, Märta and Gunnar V. Philipson Foundation, Ronald McDonald Barnfond, Harald and Greta Jeanssons Foundation, Magnus Bergvalls Foundation, the Russian Foundation for Basic Research, and INTAS grant 97-11404.

References

Alberts B, Bray D, Lewis J, Raff M, Roberts K, Watson JD (1994) Molecular biology of the cell, 3rd edn. Garland, New York

Chen PY, Pearce D, Verkman AS (1988) Membrane water and solute permeability determined quantitatively by self-quenching of an entrapped fluorophore. Biochemistry 27: 5713–5718

Crowe WE, Altamirano J, Huerto L, Alvarez-Leefmans FJ (1995) Volume changes in single N1E-115 neuroblastoma cells measured with a fluorescent probe. Neuroscience 69: 283–296

Deen PM, Rijss JP, Mulders SM, Errington RJ, van Baal J, van Os CH (1997) Aquaporin-2 transfection of Madin-Darby canine kidney cells reconstitutes vasopressin-regulated transcellular osmotic water transport. J Am Soc Nephrol 8: 1493–1501

Echevarria M, Verkman AS (1992) Optical measurement of osmotic water transport in cultured cells. Role of glucose transporters. J Gen Physiol 99: 573–589

Farinas J, Verkman AS (1996) Cell volume and plasma membrane osmotic water permeability in epithelial cell layers measured by interferometry. Biophys J 71: 3511–3522

Farinas J, Simanek V, Verkman AS (1995) Cell volume measured by total internal reflection microfluorimetry: application to water and solute transport in cells transfected with water channel homologs. Biophys J 68: 1613–1620

Farinas J, Kneen M, Moore M, Verkman AS (1997) Plasma membrane water permeability of cultured cells and epithelia measured by light microscopy with spatial filtering. J Gen Physiol 110: 283–296

Finkelstein A (1987) Water movement through lipid bilayers, pores, and plasma membranes: theory and reality. Wiley, New York

Fischbarg J, Kuang KY, Hirsch J, Lecuona S, Rogozinski L, Silverstein SC, Loike J (1989) Evidence that the glucose transporter serves as a water channel in J774 macrophages. Proc Natl Acad Sci USA 86: 8397–8401

Fournier I, Barwicz J, Tancrede P (1998) The structuring effects of amphotericin B on pure and ergosterol- or cholesterol-containing dipalmitoylphosphatidylcholine bilayers: a differential scanning calorimetry study. Biochim Biophys Acta 1373: 76–86

Gilmore JA, McGann LE, Liu J, Gao DY, Peter AT, Kleinhans FW, Critser JK (1995) Effect of cryoprotectant solutes on water permeability of human spermatozoa. Biol Reprod 53: 985–995

Giocondi M-C, Friedlander G, Le Grimellec C (1990) ADH modulates plasma membrane lipid order of living MDCK cells via a cAMP-dependent process. Am J Physiol 259: F95–F103

Heeswijk MP van, Os CH van (1986) Osmotic water permeabilities of brush border and basolateral membrane vesicles from rat renal cortex and small intestine. J Membr Biol 92: 183–193

Kao HP, Verkman AS (1994) Tracking of single fluorescent particles in three dimensions: use of cylindrical optics to encode particle position. Biophys J 67: 1291–1300

King LS, Agre P (1996) Pathophysiology of the aquaporin water channels. Annu Rev Physiol 58: 619–648

Knepper MA, Verbalis JG, Nielsen S (1997) Role of aquaporins in water balance disorders. Curr Opin Nephrol Hypertens 6: 367–371

Lopes AG, Guggino WB (1987) Volume regulation in the early proximal tubule of the Necturus kidney. J Membr Biol 97: 117–125

McManus M, Fischbarg J, Sun A, Hebert S, Strange K (1993) Laser light-scattering system for studying cell volume regulation and membrane transport processes. Am J Physiol 265: C562–C570

Meyer MM, Verkman AS (1987) Evidence for water channels in renal proximal tubule cell membranes. J Membr Biol 96: 107–119

Oliet SH, Bourque CW (1993) Mechanosensitive channels transduce osmosensitivity in supraoptic neurons. Nature 364: 341–343

Park JH, Saier MH (1996) Phylogenetic characterization of the MIP family of transmembrane channel proteins. J Membr Biol 153: 171–180

Roberts SK, Yano M, Ueno Y, Pham L, Alpini G, Agre P, LaRusso NF (1994) Cholangiocytes express the aquaporin CHIP and transport water via a channel-mediated mechanism. Proc Natl Acad Sci USA 91: 13009–13013

Sasaki S, Ishibashi K, Marumo F (1998) Aquaporin-2 and -3: representatives of two subgroups of the aquaporin family colocalized in the kidney collecting duct. Annu Rev Physiol 60: 199–220

Srinivas SP, Bonanno JA (1997) Measurement of changes in cell volume based on fluorescence quenching. Am J Physiol 272: C1405–C1414

Tauc M, Le Maout S, Poujeol P (1990) Fluorescent video-microscopy study of regulatory volume decrease in primary culture of rabbit proximal convoluted tubule. Biochim Biophys Acta 1052: 278–284

Valenti G, Frigeri A, Ronco PM, D'Ettorre C, Svelto M (1996) Expression and fuctional analysis of water channels in a stably AQP2-transfected human collecting duct cell line. J Biol Chem 271: 24365–24370

Verkman AS, van Hoek AN, Ma T, Frigeri A, Skach WR, Mitra A, Tamarappoo BK, Farinas J (1996) Water transport across mammalian cell membranes. Am J Physiol 270: C12–C30

Wintour EM (1997) Water channels and urea transporters. Clin Exp Pharmacol Physiol 24: 1–9

Yano M, Marinelli RA, Roberts SK, Balan V, Pham L, Tarara JE, de Groen PC, LaRusso NF (1996) Rat hepatocytes transport water mainly via a non-channel-mediated pathway. J Biol Chem 271: 6702–6707

Yu ZW, Quinn PJ (1998) Solvation effects of dimethyl sulphoxide on the structure of phospholipid bilayers. Biophys Chem 70: 35–39

Zhang RB, Logee KA, Verkman AS (1990) Expression of mRNA coding for kidney and red cell water channels in *Xenopus* oocytes. J Biol Chem 265: 15375–15378